ON THE HYSTERETIC CHARACTERISTICS OF THE WIND-STRUCTURE INTERACTION

Migdonia GEORGESCU [1] , Ligia MUNTEANU [2]
[1] National Museum of Romanian History, Bucharest
[2] Institute of Solid Mechanics, Romanian Academy, Bucharest

The purpose of research is to analyze the hysteretic nature of the wind-structure interaction for a structure. As a case study, a structure with rectangular profile is considered, namely the Bella hotel from Copenhagen. The model was tested in the virtual wind tunnel executed with the CFDS (Computational Fluid Dynamics Simulation) Version 1.0Beta1 pentru 2D intitulat*:* The Java Virtual Wind Tunnel. The results show that the hysteretic behavior of the structure is characterized by changes into the model of the air density, the normal and axial velocities of the wind, the local average pressure coefficients and the total average pressure coefficients, during the flow.

Key words: Wind-structure interaction, flow, wind-tunnel.

1. INTRODUCTION

The interaction between the structure and the action of the wind depends essentially on the nature of the air movement and the topography and shape of the structure. While the incidence of the wind direction on a structure favors the formation of vortices, the phenomenon of aeroelasticity instability is developed in the direction perpendicular to the wind direction. Instabilities arising in the slender aerodynamical structures are due to the forced cyclic oscillations. The phenomenon is called flutter. Forced vibrations lead to fatigue failure, such as the Tacoma-Narrows Bridge in US which collapsed in 1940 due to the action of a 64 km/h wind. In 2012, the wind struck our coast several times, to more than 80km/h, provoking considerable material damage.

In this paper the nature of the hysteretic behavior of the structures subjected to wind actions is investigated. As a case study, we consider a structure with rectangular profile, namely the Bella hotel from Copenhagen. This structure was analyses in [1], along with other types of structures with different shapes, i.e. pyramidal, parabolic with triangular peak, truncated hyperbolic and churches, respectively.

Fig.1. A rectangular structure - Bella Hotel from Copenhagen.

Investigation of structure shape effects on structural response is an important subject for understanding the hysteretic behaviour of the structures under the wind action. The architect Frank Lloyd Wright said that the form follows the function [2]. With this respect, the modeling of structures subjected to wind action should take into account the relationship between form and function [3], [4]. Several models of structures with different shapes inspired by real world can be constructed based on ideas of Weiss [3].

2. PROBLEM FORMULATION

The wind-structure interaction occurs when the wind movement causes deformation of the structure. This deformation, in turn, changes the boundary conditions of the fluid [5]-[14].

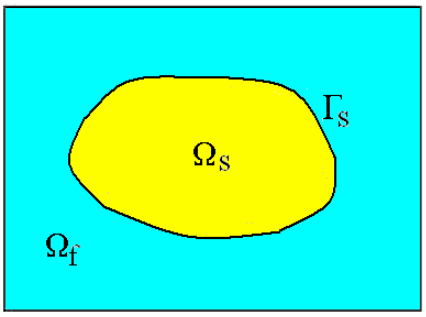

Fig. 2. Computational domain.

The computational domain $\Omega = \bar{\Omega}_s \cup \bar{\Omega}_f$ of boundary Γ, is composed of two subdomains, namely a structural subdomain $\bar{\Omega}_s$ which contains the structure subjected to the action of wind, and a subdomain $\bar{\Omega}_f$ where the wind is acting (Fig. 2). The boundary between $\bar{\Omega}_s$ and $\bar{\Omega}_f$ is $\Gamma_s = \bar{\Omega}_s \cap \bar{\Omega}_f$. D'Alembert principle leads to the motion equations for the solid in the Lagrange system of reference

$$\rho_s \frac{\partial}{\partial t} v_{si} - \sigma_{sij,j} + f_{si} = 0 \text{, in } \bar{\Omega}_s \text{,} \tag{1}$$

where ρ_s is the solid density. The index s designates the solid, $v_{si} = \frac{\partial}{\partial t} u_{si}$ are the components of the velocity vector which are expressed as partial derivatives of the displacement field u_{si}, $i = 1,2,3$, σ_{sij}, $i, j = 1,2,3$ are the components of the stress tensor, and f_{si} are the body forces. We use the convention of the summation with respect to repeated indices. The constitutive Hooke law is

$$\sigma_{sij} = \lambda \delta_{ij} \varepsilon_{sll} + 2G\varepsilon_{sij} \text{, in } \bar{\Omega}_s \text{ ,} \tag{2}$$

where $\varepsilon_{sij} = 1/2(u_{si,j} + u_{sj,i})$ are components of the strain tensor, and λ, G, are Lamé elastic constants

$$G = \frac{E}{2(1+\nu)}, \quad \lambda = \frac{E\nu}{(1+\nu)(1-2\nu)}, \tag{3}$$

with E the Young modulus, and ν Poisson's ratio. Substituting (2) into (1) the motion equations in displacements are obtained

$$\rho_s \frac{\partial^2}{\partial t^2} u_{sk} = (\lambda + G) u_{l,lk} + G u_{k,ll} + \rho_s f_{sk} \text{ , } k = 1,2,3 \text{ , în } \bar{\Omega}_s \text{.} \tag{4}$$

For the behavior of the wind motion, the *Reynolds* equations are considered. These equations are obtained from the Navier-Stokes equations by decomposition

$$u = \overline{u} + u' \ , \tag{5}$$

in which the variable u is written as a sum between a time-averaged value $\overline{u}$ and a value u' that represents the deviation (fluctuation). The average $\overline{u}$ over time of the variable v for large enough T, is given [7], [8]

$$< u >_t = \overline{u} = \frac{1}{T} \int_{t-T/2}^{t+T/2} u(t') \mathrm{d}t' \ . \tag{6}$$

The Reynolds equations and the continuity equation are written in an Eulerian system of reference as

$$\frac{\partial(\rho \overline{v}_i)}{\partial t} + (\rho \overline{v}_i \overline{v}_j)_{,j} = -\overline{p}_{,i} + \left(\mu(\overline{v}_{i,j} + \overline{v}_{j,i}) + \tau_{ij}\right)_{,j} + f_i, \quad \text{în } \overline{\Omega}_f \tag{7}$$

$$\frac{\partial \rho}{\partial t} + \left(\rho \overline{v}_i\right)_{,i} = 0 \text{, în } \overline{\Omega}_f \ . \tag{8}$$

The Reynolds stresses τ_{ij} are expressed in the Boussinesq form

$$\tau_{ij} = -\rho \overline{v'_{,i} v'_{,j}} = \mu_t \left(\overline{v}_{i,j} + \overline{v}_{j,i}\right), \tag{9}$$

where μ_t is the turbulent viscosity of the fluid. Substituting (9) into (7) we obtain the equations in velocities

$$\frac{\partial(\rho \overline{v}_i)}{\partial t} + (\rho \overline{v}_i \overline{v}_j)_{,j} = -\overline{p}_{,i} + \left(\mu_{ef}(\overline{v}_{i,j} + \overline{v}_{j,i})\right)_{,j} + f_i \text{, în } \overline{\Omega}_f \text{,} \tag{10}$$

with $\mu_{ef} = \mu + \mu_t$. On the boundary solid-fluid Γ_s, the Dirichlet are Neumann conditions are considered in order to remove the slipping between the constituents

$$v_{si} = \overline{v}_{fi} \text{,} \quad i = 1,2,3 \text{,} \quad \text{on } \Gamma_s \text{,} \tag{11}$$

$$\sigma_{sij} n_i = \sigma_{fij} n_i \ \text{,} \quad j = 1,2,3 \text{,} \quad \text{on } \Gamma_s \ . \tag{12}$$

The condition (12) can be written in term of the continuity of displacements on Γ_s

$$u_{si} = u_{fi} \text{,} \ i = 1,2,3 \text{, on } \Gamma_s \ . \tag{13}$$

The complete set of equations that discribe the interaction wind-structure is

$$\rho_s \frac{\partial^2}{\partial t^2} u_{sk} = (\lambda_s + G_s) u_{sl,lk} + G_s u_{sk,ll} + \rho_s f_{sk} \text{,} \ k = 1,2,3 \text{, in } \overline{\Omega}_s$$

$$\frac{\partial(\rho_f \overline{v}_{fi})}{\partial t} + (\rho_f \overline{v}_{fi} \overline{v}_{fj})_{,j} = -\overline{p}_{f,i} + \left(\mu_{fef}(\overline{v}_{fi,j} + \overline{v}_{fj,i})\right)_{,j} + f_{fi} \text{,} \ i = 1,2,3 \text{, in } \overline{\Omega}_f$$

$$\frac{\partial \rho_f}{\partial t} + \left(\rho_f \overline{v}_{fi}\right)_{,i} = 0 \ \text{ in } \overline{\Omega}_f \ . \tag{14}$$

$$v_{si} = v_{fi} \quad \text{on } \Gamma_s \text{,} \ \ i = 1,2,3 \text{,}$$

$$u_{si} = u_{fi} \quad \text{on } \Gamma_s \text{,} \quad i = 1,2,3 \ .$$

where $v_{si}=\frac{\partial}{\partial t}u_{si}$, $v_{fi}=\frac{\partial}{\partial t}u_{fi}$ and $\overline{v}_{fi}=\frac{1}{T}\int_{t-T/2}^{t+T/2}v_{fi}(t')\mathrm{d}t'$. The unknowns of these equations are

$$U_k(x,t)=\{u_{s1},u_{s2},u_{s3},v_{f1},v_{f2},v_{f3},p_f\},\ \ k=1,2,3...,7\,. \tag{15}$$

.

3. RESULTS

Theoretical results obtained by solving the complete set of wind-structure interaction equations (14) and (15) are verified by specialized software that simulate the virtual wind tunnel. It is the software CFDS (Computational Fluid Dynamics Simulation) Version 1.0Beta1 for 2D, titled: Java Virtual Wind Tunnel. The software was developed at the Massachusetts Institute of Technology and is based on the rules ASCE American Society of Civil Engineering Wind Tunnel Testing for Buildings and Other Structures (ASCE 7-10). Fig. 1 shows the flow visualization around the 1/100 scale model in the real wind tunnel executed with the XFlow CFD. The airflow speed is in the range of values from 2 to 20 [s^{-1}]. Duration of the experiment is 12 seconds. Fig. 3 represents the flow visualization around the hotel after 3 seconds, while Fig. 4, after 10 seconds, respectively.

The map of local average pressure coefficients C_p to which p_s are multiplied to obtain the static wind pressure at any point on the building, according to

$$\overline{p}_f(z)=C_p(z)p_s(z)=\frac{1}{2}C_p(z)\rho V^2(z)=1,2047C_p(z)V^2(z)\,. \tag{16}$$

These coefficients take values in the range of -2 and 1. In our study, both hotel buildings are considered together. They are inclined to the horizontal axis with 15^0 one in a direction and the other in the opposite direction. We consider $H=90\,\mathrm{m}$ and $2b=30\,\mathrm{m}$. Local average pressure coefficients C_p corresponding to these buildings shown in Fig. 5 were used as experimental data $U_m^{\exp}=C_{pm}$, $m=1,2,...,M$, $M=100$. This data is sufficient to determine the unknowns α_{km}, k_{kmj}, γ_{km}, λ_{km}, C_{km}, $k=1,2,...,7$, $m=1,2$, $j=1,2,3$, from a genetic algorithm.

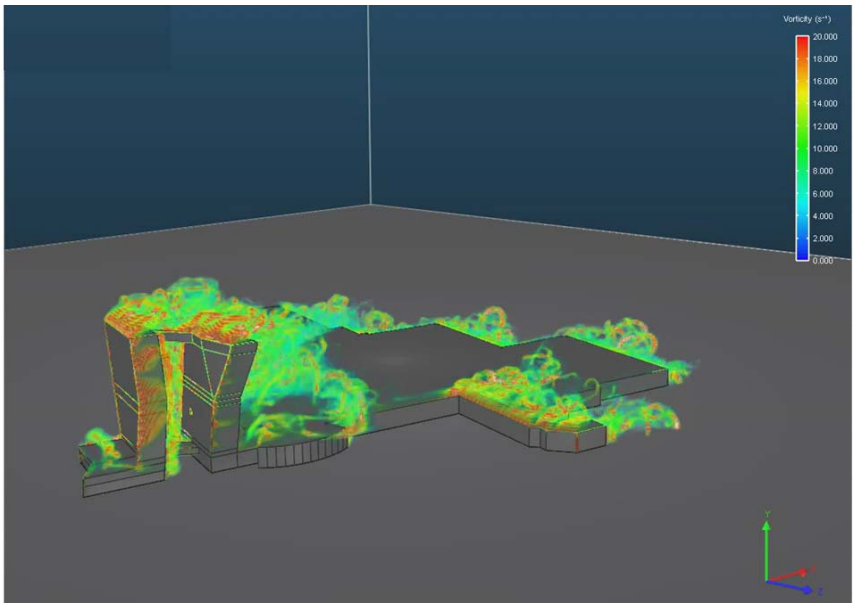

Fig. 3. Flow visualization around the Bella hotel after 3 seconds.

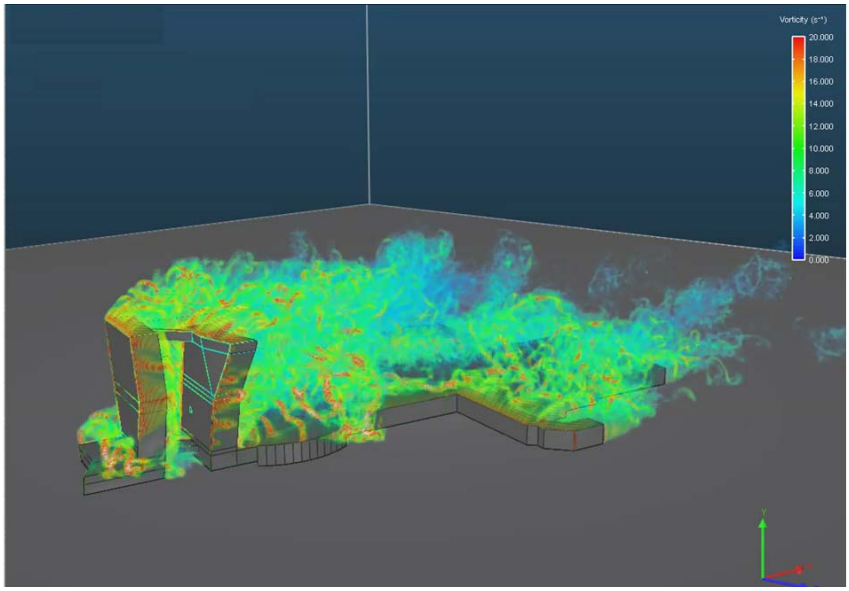

Fig. 4. Flow visualization around the Bella hotel after 10 seconds.

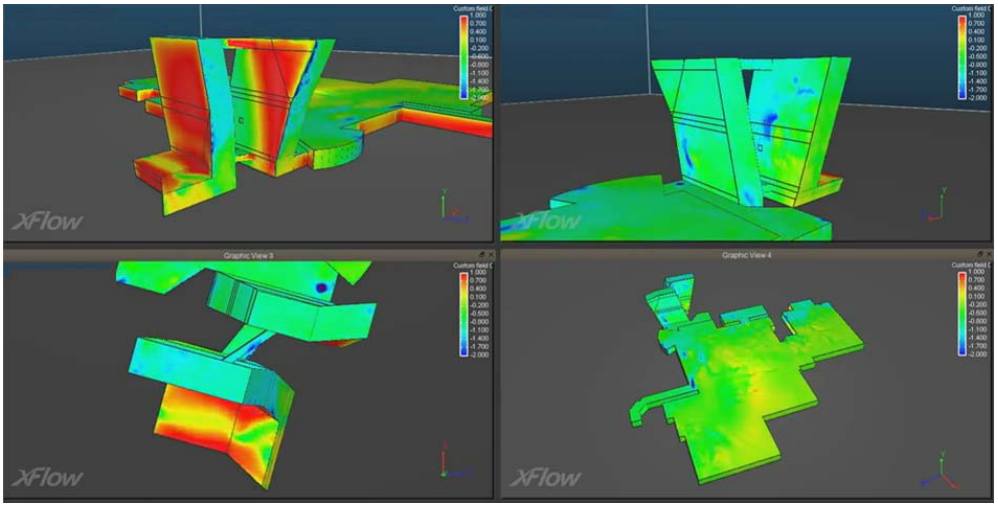

Fig. 5. Local average pressure coefficients C_p used as experimental data for genetic algorithm.

We report the first results relating to the solid surface displacements. Figs. 6-8 give the variation of u_{si}/u_0, $i=1,2,3$, with u_0 a reference displacement, against z/H for 5 values of the wind speed 80, 70, 68, 50 and 10m/s, respectively ($Ma=0{,}235$; 0,2; 0,199; 0,146 and 0,029).

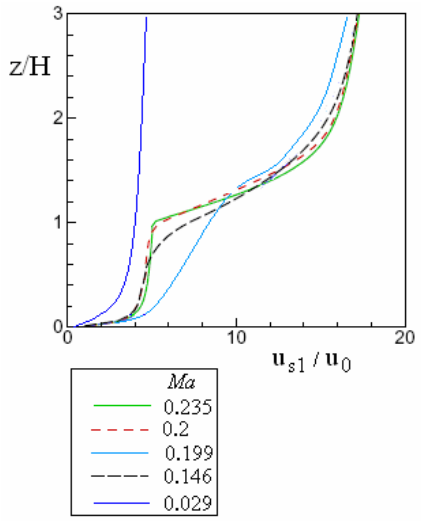

Fig.6. Dimensionless variation of u_{s1}/u_0 against z/H.

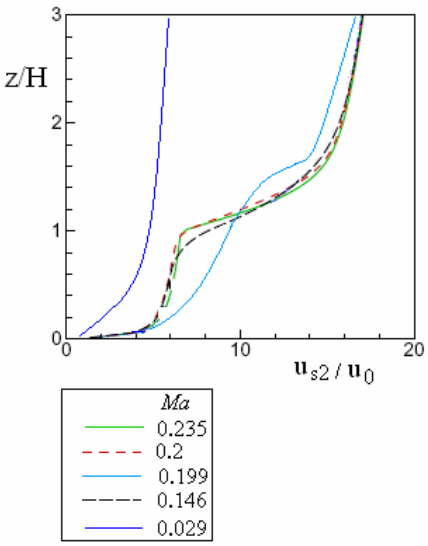

Fig. 7. Dimensionless variation of u_{s2}/u_0 against z/H.

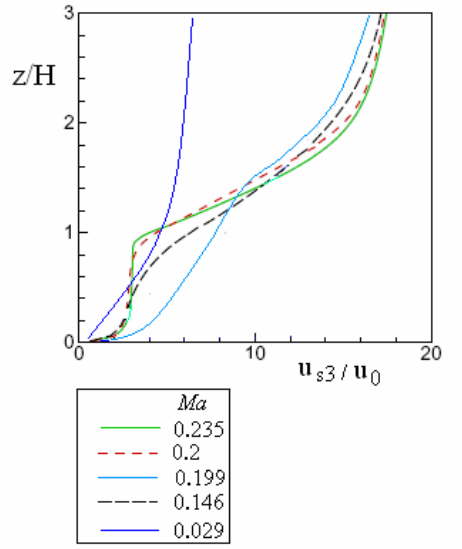

Fig. 8. Dimensionless variation of u_{s3}/u_0 against z/H.

Theoretical values of the local average pressure coefficients C_p are presented in Fig. 9, after 10s, 20 s, and 30 s, respectively, after starting of the interaction simulation.

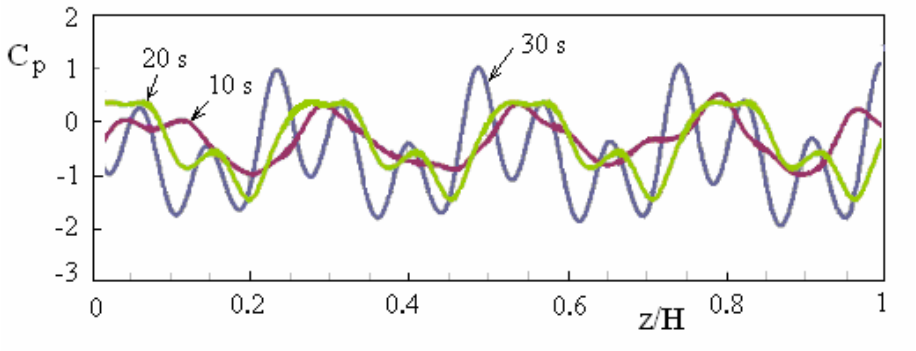

Fig. 9. Theoretical values of the local average pressure coefficient C_p.

The values of the local average pressure coefficients C_p for both buildings, on the surfaces located perpendicular to the air flow, with respect to z/H are presented in Fig. 10.

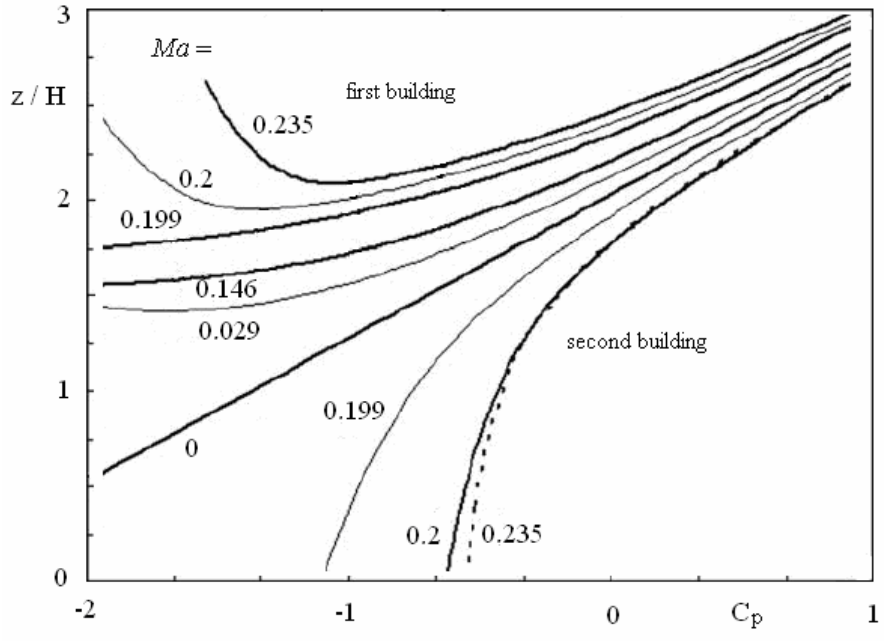

Fig. 10. Variation of the local average pressure coefficient C_p for both buildings, against z/H.

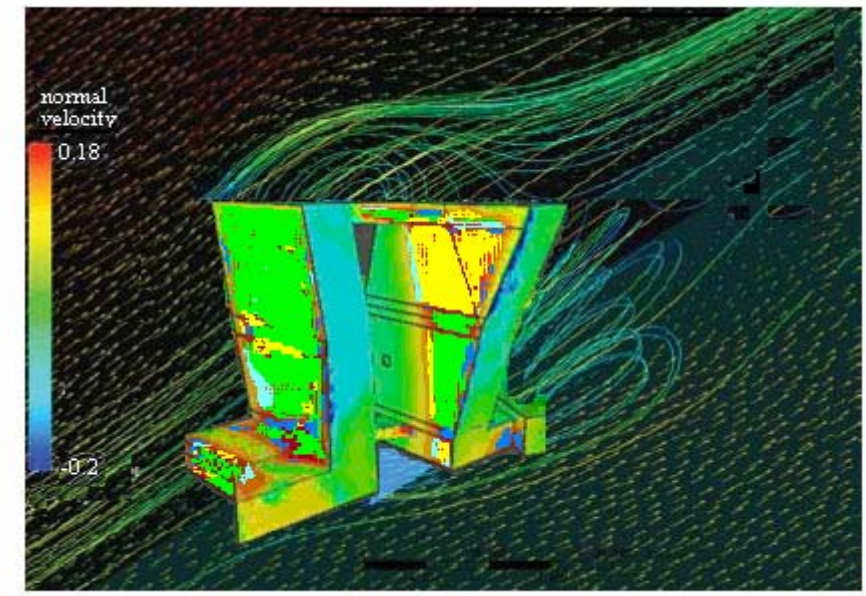

Fig. 11. Profile of the normal velocity.

The normal velocity profile is presented in Fig. 11. Fig. 12 displays the profile of the local average pressure coefficient C_p. As verification we see that C_p takes values between -2 and 1, while C_{pt} takes values between 0 and 3.

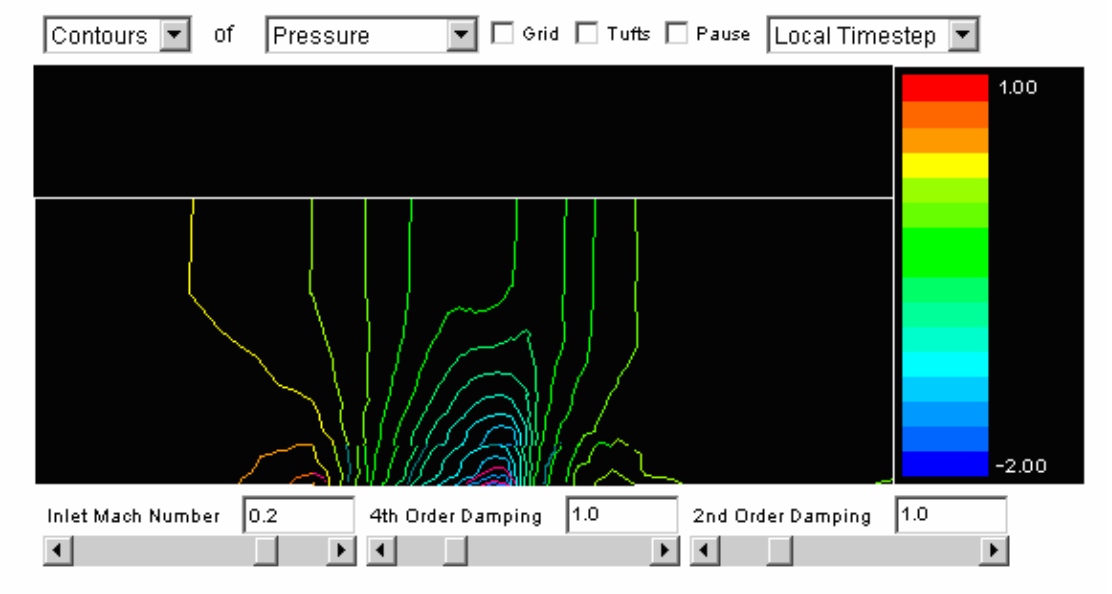

Fig. 12. Profile of the local average pressure coefficient C_p, on the building surface.

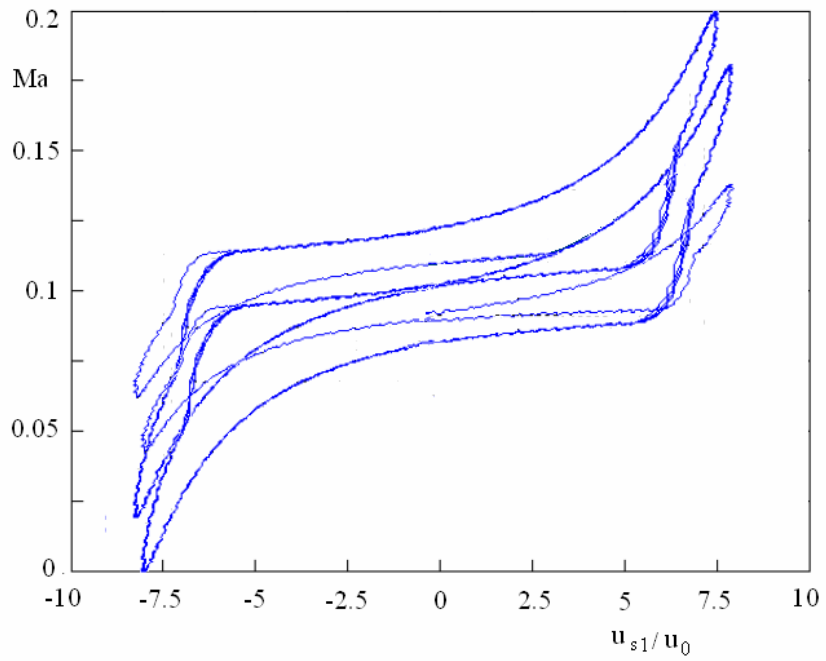

Fig. 13. Hysteretic loop u_{s12}/u_0 against the Mac number.

The hysteretic loops of dimensionless solid displacement u_{si}/u_0, $i=1,2,3$ in the top of the building, against the Mac number, are shown in Figs. 14-16. The shape of the curves is similar showing not only the dependence of the building on the speed of the air motion represented by the Mac number, but also on its past states. The hysteretic behavior is characterized by changes into the model of the air density, normal and axial velocities of the wind, the local average pressure coefficients C_p, and the total average pressure coefficients C_{pt}, during the flow. The model was tested in the virtual wind tunnel executed with the CFDS.

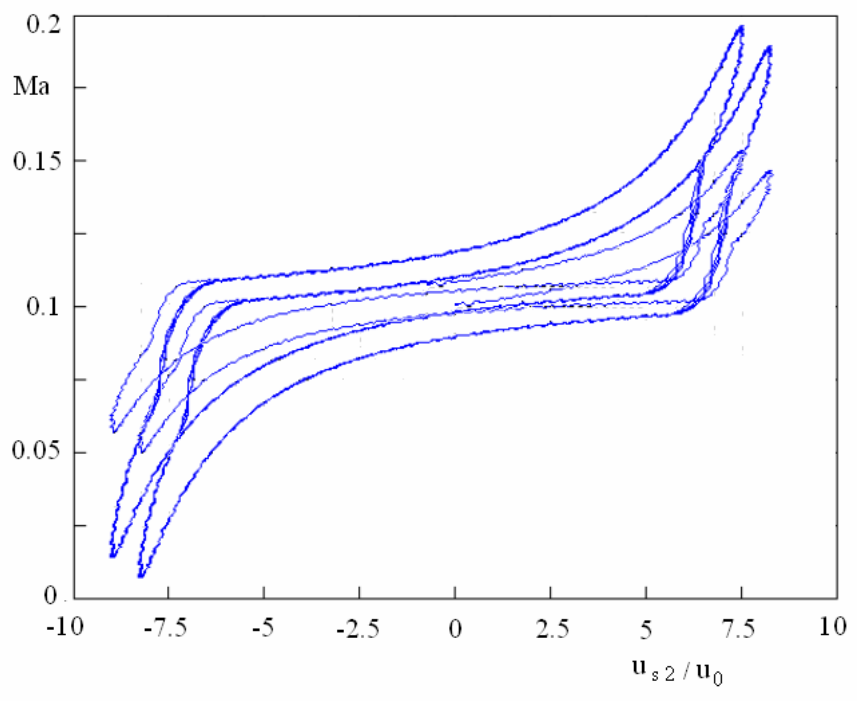

Fig. 14. Hysteretic loop u_{s2}/u_0 against the Mac

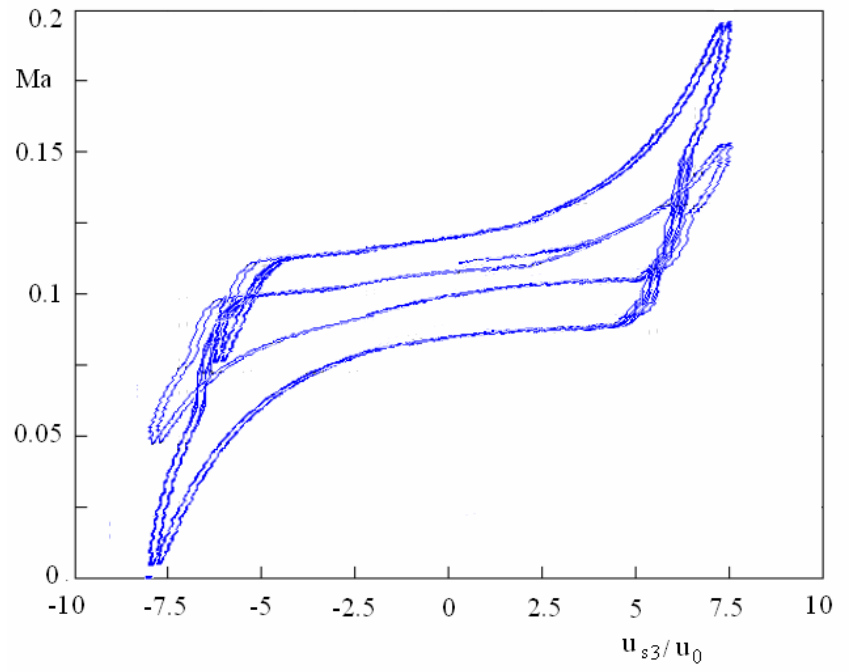

Fig. 15. Hysteretic loop u_{s3}/u_0 against the Mac number.

5. CONCLUSIONS

This paper has analyzed the hysteretic nature of the wind-structure interaction for a structure. As a case study, a structure with rectangular profile is considered, namely the Bella hotel from Copenhagen. The model was tested in the virtual wind tunnel executed with the CFDS. The hysteretic behavior of the structure is characterized by changes into the model of the air density, normal and axial velocities of the wind and the local average pressure coefficient C_p, during the flow. Let us note that the local average pressure

coefficients C_p and of the total average pressure coefficients C_{pt}, respectively are determined by solving the problem of interaction theory given by (14) and (15). Meanwhile, CFDS provides full behavior of these coefficients. In this context, the coefficients and can be considered indicators of verifying of the theoretical results by comparing them with own data.

Acknowledgement. The authors acknowledge the similar and equal contributions to this article

REFERENCES

1. GEORGESCU, M., *Răspunsul dinamic al struturilor cu comportament elastic la acţiunea vânturilor, vârtejurilor şi a rafalelor*, Teza doctorat, Institutul de Mecanica Solidelor, Bucureşti 2013.
2. THOMSON, I., *Frank Lloyd Wright: A Visual Encyclopedia,* London: PRC Publishing Ltd., 2002Thomson 2002.
3. WEISS, M.D., *The influence of shape and form on the wibd-related engineering properties of tall buildings under simulated lateral wind loads*, PhD thesis, The Faculty of the School of Engineering and Applied Science University of Virginia, 1997.
4. MERRICK, R., BITSUAMLAK, G., *Shape effects on the wind-induced response of high-rise buildings*, Journal of Wind and Engineeringm 6(2), 1–18, 2009.
5. DALGLIESH, W.A., W.R.SCHRIEVER, *Wind Pressures On Buildings*, National Research Council Canada 1968.
6, DAVENPORT, A.G., *A Rationale for the Determination of Design Wind Velocities,* Proceedings ASCE Structural Division, 86, 139-66, 1960
7. PIELKE, R.A., *Mesoscale Meteorological Modeling*. Academic Press, Dordrecht, 1984.
8. POPE, S.B., *Turbulent Flows*. Cambridge University Press, Cambridge, 2000.
9. DAVENPORT, A.G., *The Application of Statistical Concepts to the Wind Loading of Structures*, Proc. Institution of Civil Engrs. 19, 449-472, 1961.
10. DAVENPORT, A.G., *The Relationship of Wind Structure to Wind Loading*, Proc. Symp. Wind Effects on Buildings and Structures, Nat. Phys. Lab., Teddington, UK, 1, 53-102, 1965.
11. DAVENPORT, A.G., SURRY, D., STATHOPOULOS, T., *Wind Loads on Low-rise Buildings*, Final Rep. on Phases I and *II*, BLWT-SS8-1977, Univ. Western Ontario, London, Ontario, Canada, 1977.
12. DAVIDSON, L., *An Introduction to Turbulence Models.* Report 97/2, Dept. of Thermo and Fluid Dynamics, Chalmers,
13. ENDO, E., KURABUCHI, T., ISHII, M>, KOMAMURA, K., MARUTA, E., SAWACHI, T., *Study on the numerical predictive accuracy of wind pressure distribution and air flow characteristics. Part 1: Optimization of turbulence models for practical use* – International Conference "Passive and Low Energy Cooling for the Built Environment", Santorini, Greece, 77–82, 2005.
14. FARQUHAR, S., KOPP, G.A., SURRY, D., *Wind Tunnel and Uniform Pressure Tests of a Standing Seam Metal Roof Model*, Journal of Structural Engineering, ASCE April 2005, 650–659, 2005.